ACCEPTED MANUSCRIPT
Journal of Applied Physics
AIP Publishing
This is the author's peer reviewed, accepted manuscript. However, the online version of record will be different from this version once it has been copyedited and typeset.
PLEASE CITE THIS ARTICLE AS DOI: 10.1063/5.0005775

# Controlling the crystallization of Nd-doped $Bi_4Ti_3O_{12}$ thin-films for lead-free energy storage capacitors

D. P. Song,[1,2,a)] J. Yang,[3] J. X. Sun,[1] L. -Y. Chen,[1] Y. Q. Chu,[1] Y. Wang,[1] and J. -K. Lee[2,b)]
[1)] *Department of Physics, Jiangsu University of Science and Technology, Zhenjiang 212003, China*
[2)] *Department of Mechanical Engineering and Material Science, University of Pittsburgh, PA, 15261, USA*
[3)] *School of Materials science and Engineering, Jiangsu University of Science and Technology, Zhenjiang 212003, China*

(Dated: 1 May 2020)

Environmental benign non-lead-based dielectric thin-film capacitors with high electrostatic energy density, long-term stability, and fast charge/discharge capability are strongly demanded in advanced electrical and pulsed power devices. Here, we propose that insufficient crystallization is an effective method to achieve high energy storage performance. A high efficiency of 84.3%, together with a good energy density of 41.6 J/cm$^3$ and an excellent fatigue endurance, is obtained in lead-free Nd-doped $Bi_4Ti_3O_{12}$ (BNT) film of low crystallization. An increase in the annealing temperature increases the crystallinity and grain size, which improves the ferroelectric polarization of thin film. A narrow hysteresis loop with large maximum polarization and small remnant polarization is obtained in the insufficiently crystallized film which is annealed in the intermediate temperature. This film also show lower leakage current compared with the fully crystallized counterpart, due to the less defective microstructure. This work provides a straightforward and executable method to design ferroelectric materials for the applications of energy storage capacitors.

## I. INTRODUCTION

Dielectric capacitors that store energy in the form of electric fields are widely used in pulse electronic devices because of an extremely short period of discharge time and a very intense pulsed current.[1,2] For the dielectrics with high permittivity, the recoverable energy storage density ($U_{re}$) can be expressed as: $U_{re} = \int_{P_r}^{P_s} EdP$, where the $P$, $E$, $P_m$ and $P_r$ represent the polarization, electric field, maximum polarization and remnant polarization.[3] $U_{re}$ becomes large for materials of larger $P_m$ and smaller $P_r$. In paraelectric materials, $P_r$ is zero but $P_m$ is also small. While $P_m$ is large in ferroelectrics, $P_r$ is also large. It seems difficult to control one of them individually. In addition, materials of higher polarization values (or permittivity) usually have low electric field tolerance (also called breakdown electric field $E_b$) which should be large for the energy storage application.

There are several ways to address the intrinsic material problems and improve the energy storage performance: i) to improve $E_b$ of materials of large $P_m$ such as ferroelectric ceramics;[4] ii) to enhance the polarization of materials of large $E_b$ such as dielectric polymer;[5] iii) to mix materials of large $E_b$ with materials of large $P_m$.[6] The third method (i.e. the mixture design) attracts a considerable amount of interest. Usually, ceramic particles/fibers are added into the polymer matrix for the energy storage application. However, the design and processing of high-performance mixture is complicated because it requires precise controlling of the dispersion of the second phase and the interface between the matrix and the second phase.[7] This difficulty in the mixture design suggests that it is very desirable to find single-phase materials that have large $E_b$ as well as large $P_m$.

Compared to bulk ceramics, thin films show much larger $E_b$ because of their smaller grain size, denser microstructure and smaller thickness.[8] Combine with the intrinsic large polarization value, the ferroelectrics thin film capacitors have attracted an increasing attention recently. If $P_r$ of ferroelectrics thin film can be reduced, this series of materials is ideal for the energy storage devices. Several groups have studied the energy storage performance of perovskite $ABO_3$ type ferroelectrics containing Pb- and Ba-ions.[9,10] Lee et al. and Sun et al. have reported the Pb- and Ba-based thin film capacitors of La-doped $PbZrO_3$ (PLZO) and Zr-doped $BaTiO_3$ (BZTO) systems.[11,12] $U_{re}$ of PLZO and BZTO thin film capacitors are 15.2 J/cm$^3$ and 30.4 J/cm$^3$ at 1 MV/cm and 3 MV/cm, respectively. Correspondingly, the energy storage efficiency ($\eta$) is 74.1% and 81.7%. Furthermore, Yang et al. reported maximum recoverable energy storage density of 68.5 J/cm$^3$, but $\eta$ of 52.9% in doped $Na_{0.5}Bi_{0.5}TiO_3$-based thin film capacitors which have higher $E_b$ by controlling Bi content.[13] The same group reported another $Na_{0.5}Bi_{0.5}TiO_3$-based film capacitor of the giant and stable energy storage capability.[14,15] The ultrahigh $U_{re}$ of 60-150 J/cm$^3$ is also demonstrated in $BiFeO_3$-based (BFO) ferroelectric capacitors from both experimental and theoretical studies.[1,16,17] Although much of them exhibit good temperature stability, their fatigue resistance and energy efficiency need to be further improved.

Bismuth-base layered perovskite (also called Aurivillius phase AP) compounds, known as a type of fatigue-free ferroelectric materials, have large spontaneous polarization, relatively high $E_b$ and high Curie temperature.[18] AP thin films meet all materials requirements for the energy storage application except low $P_r$. Yang et al. reported multi-layered structures which consisting of BFO and AP thin films. They exhibited good energy storage performance and excellent fatigue

[a)] Electronic mail: dpsong@just.edu.cn
[b)] Electronic mail: jul37@pitt.edu

Journal of Applied Physics
ACCEPTED MANUSCRIPT
This is the author's peer reviewed, accepted manuscript. However, the online version of record will be different from this version once it has been copyedited and typeset.
PLEASE CITE THIS ARTICLE AS DOI: 10.1063/5.0005775
AIP Publishing



resistance.[19] In addition, relaxation behaviors resulting from the lattice distortion and structural transformation by rare element doping into four-layered AP films increased energy storage performances.[20] In recent studies, both multi-layered structures and element doping can effectively reduce the remnant polarization of the thin films.

In this work, the remnant polarization of a prototypical AP thin film ($Bi_{3.15}Nd_{0.85}Ti_3O_{12}$ BNT) which are annealed at different temperature has been thoroughly and systematically researched because the thermal annealing has a significant effect on the ferroelectric property-structure relationship of thin films.[21] Here, we report that a change in the annealing temperature significantly changes the remnant polarization of BNT thin films. High temperature (700 °C) annealed films exhibit a typical ferroelectric hysteresis loop of large $P_m$ and $P_r$ similar to those previously reported.[22] However, thin films annealed at the moderate temperature (650 °C) show a slender hysteresis loop of large maximum polarization ($\sim$ 50 $\mu$C/cm) and small remnant polarization ($\sim$ 5.7 $\mu$C/cm). The smaller remnant polarization is related to their dense morphology with nanocrystal grains and smooth surface. Such a slim polarization loop of BNT thin film leads to large $U_{re}$ (41.6 J/cm$^3$) and high $\eta$ (84.3%). Furthermore, the fatigue and temperature resistance suggest that BNT thin films can be used as a ferroelectric capacitor matrix.

## II. EXPERIMENTAL

All BNT thin films were prepared by chemical solution deposition method on the platinum-coated silicon substrate. The precursor composed of stoichiometric metal cationic and propionic acid was spin-coated and pyrolyzed to form amorphous precursor films. Metal cationic sources were bismuth (III) acetate with 5% mol excess, neodymium (III) acetate, and tetrabutyl titanate. The spin coating were done at a rotation speed of 5000 rpm and for a duration time of 20 s. Then it was baked at temperature of 400 °C for 10 min. After this process was repeated 12 times to increase the film thickness to around 450 nm, the pyrolyzed films were crystallized at different temperatures from 550 to 700 °C. For brevity, thin films annealed at 550, 600, 650 and 700 °C are named as BNT55, BNT60, BNT65 and BNT70, respectively. A Philips XPert PRO X-ray diffractometer (XRD, a Philips Xpert Pro diffractometer, Holland) with Cu-K radiation and a Raman spectrometer with a 532 nm excitation laser (Renishaw inVia, England) were used to determine the structures of BNT films at room-temperature (RT). Microstructure and thickness of films were examined using field-emission scanning electron microscopy (FE-SEM, FEI Sirion 200 type, Japan). Au top electrodes of 0.2 mm in diameter were deposited by a sputter (SCB-12 type Miriam small ion sputter, China) onto thin films surfaces through a shadow mask for electric measurement. Room-temperature dielectric properties were measured in the frequency range of 20 Hz - 1 MHz using a driving voltage of 1 V by a precision LCR meter (TH2828/A/S model, China). The ferroelectric and leakage properties were investigated using a Sawyer-Tower circuit attached to a computer-controlled standardized ferroelectric test system (Precision Premier II, Radiant Technologies, USA).

## III. RESULTS AND DISCUSSION

The XRD patterns of derived thin films annealed at different temperature are shown in Fig. 1(a), and the miller index of peaks including platinized silicon substrate is also listed. Thin films are polycrystalline feature and they have a random orientation. No secondary phase peaks are found. Peaks are indexed as an orthorhombic lattice with the space groups of $Fmmm$ which belongs to Aurivillius phase with three perovskite-like layers.[23] As the thermal annealing temperature increases, the crystallinity of films increases and the width of XRD peaks decreases. In order to confirm the crystal structure, Raman spectra of all derived samples are shown in the Fig. 1(b). The vibrational modes of Aurivillius films are classified into two sets: one is the movement of a layer-like rigid unit and the other is the internal vibrational modes of $TiO_6$ octahedron.[24] In Fig. 1(b), the vibrational modes were clearly visible and mark by the dashed vertical lines, which are labeled as $\nu_1$ (63.2 cm$^{-1}$), $\nu_2$ (153.7 cm$^{-1}$), $\nu_3$ (217.9 cm$^{-1}$), $\nu_4$ (262.4 cm$^{-1}$), $\nu_5$ (346.8 cm$^{-1}$), $\nu_6$ (553.9 cm$^{-1}$), and $\nu_7$ (847.6 cm$^{-1}$). By comparing Raman modes of bulk $Bi_4Ti_3O_{12}$, Raman modes of $\nu_3$, $\nu_4$, $\nu_5$, $\nu_6$, and $\nu_7$ are attributed to $TiO_6$ octahedron vibration. The rest modes ($\nu_1$ and $\nu_2$) are as-signed to rigid-layer modes.[25] Besides, there are only seven Raman active modes observed in BNT shown in Fig. 1(b), which is due to the overlap of the same symmetry vibrations and nanocrystal thin films with small grain size. Plan-view SEM images in the Fig. 1(c)-(f) demonstrate that thin films annealed at low temperature are small-sized nanocrystalline and the increase in the annealing temperature increases the grain size. During the thermal annealing, the nucleation and growth occur in thin films.[26] Under rapid annealing conditions, the films first nucleate rapidly and then grow. The process of grain growth is the result of continuous phagocytosis and consumption. At low temperature, there are a large number of nucleation sites in the film. As the annealing temperature increases, the nuclei grow and the microstructure becomes dense. At 700 °C, small grains disappear and only large grains are left. In addition, the constrained densification of thin films often leave voids, as shown in Fig. 1(f) of the BNT70. While the BNT65 film has a dense morphology consisting of nanocrystal grains, BNT70 films have larger grains and pores.

Dielectric constant is the important factor for the dielectric energy storage capacitors. The frequency dependence of dielectric constant ($\varepsilon_r$) and dielectric loss (tan$\delta$) of BNT films annealed at different temperature are show in Fig. 2(a). Thermal annealing at higher temperature increases $\varepsilon_r$. In addition, the value of $\varepsilon_r$ is decreased as the frequency increases. $\varepsilon_r$ of BNT65 and BNT70 films as large as 260 at 1 MHz. In all samples, a loss factor (tan$\delta$) below 0.05. This loss factor of BNT films is similar to that of three-layered AP films and other higher perovskite-like Aurivillius thin films reported before.[27,28] Small decrease in $\varepsilon_r$ over increase in the fre-

ACCEPTED MANUSCRIPT
Journal of Applied Physics
AIP Publishing
This is the author's peer reviewed, accepted manuscript. However, the online version of record will be different from this version once it has been copyedited and typeset.
PLEASE CITE THIS ARTICLE AS DOI: 10.1063/5.0005775

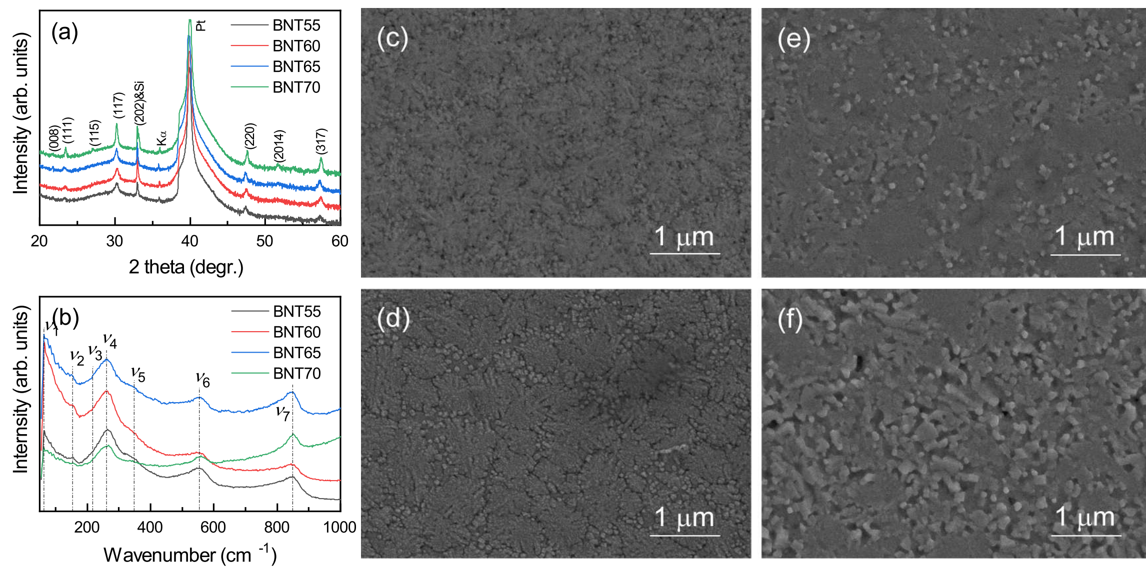


FIG. 1. (a) X-ray diffraction pattern and (b) Raman spectroscopy of BNT thin films under various annealing temperature. The SEM images of BNT thin films annealing at (c) 550, (d) 600, (e) 650 and (f) 700 Celsius.

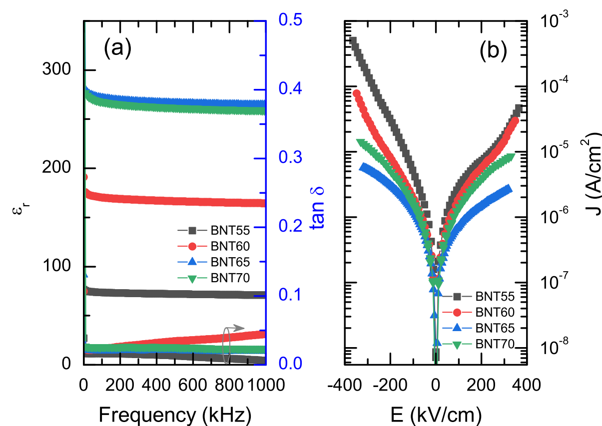


FIG. 2. (a) The frequency dependence of dielectric constant and dielectric loss for BNT films annealed at deliberately temperature. (b) The leakage current properties of all the derived thin films.

quency is attributed to a space charge effect that is suppressed at higher frequency.[29] While the grain growth at high temperature effectively enhances $\varepsilon_r$ by increasing the crystallinity, the formation of defects like oxygen vacancies at high annealing temperature decreases $\varepsilon_r$ and increase the leakage current. Fig. 2(b) shows the leakage current of all thin films. The leakage currents density $J$ continuously increases with the increase in the electric field. As the annealing temperature increases to 650 °C, the improvement of the crystallization quality decreases $J$. A further increase in the annealing temperature to 700 °C causes the formation of pores and other defects in films, which leads to high $J$ of BNT70.[23] Thus, the collective effect of the grain size and defects controls the dielectric properties and leakage current of BNT thin films which are annealed at different annealing temperature.

Fig. 3(a) shows $P$-$E$ loops of all BNT thin films at 5 kHz. As the annealing temperature increases, the shape of the hysteresis loops changes from a banana-type to an $S$-type. This confirm that the ferroelectricity is enhanced by increasing the annealing temperature. The maximum polarization at a given electric field increases as the annealing temperature increases. This is consistent with an effect of the annealing temperature on the permittivity. $P_m$ and $P_r$ of four BNT films extracted from the $P$-$E$ loops are 34.3, 42.9, 51.3, 59.9 $\mu$C/cm$^2$ and 8.9, 10.5, 6.6, 20.6 $\mu$C/cm$^2$, respectively. The ferroelectric hysteresis loop and $P_r$ of BNT70 thin film in this study are comparable to the previous results, which further confirm the high quality of the thin films.[22] Among several factors evaluating the energy-storage performance, the energy-storage density is the most important one.[8] Here polarization-based methods are employed to obtain the energy-storage density of all BNT thin films as show in the Fig. 3(b). In such a method an energy-storage density ($U$) is calculated by integrating the polarization of $P$-$E$ loop, $U = \int_0^{P_s} EdP$. According to the energy storage density formula, the calculated $U$ of four BNT thin films before breakdown electric field is given in the Table I. In addition, the $U_{re}$ ($U_{re} = \int_{P_r}^{P_s} EdP$) and energy-storage efficiency $\eta$=$U_{re}$/$U$=$U_{re}$/($U_{re}$+$U_{loss}$) are also shown in Table I. $U_{loss}$ is defined as the amount of energy density dissipated during the discharge process, as the magenta shaded area in

TABLE I. The properties of four BNT thin films before breakdown electric field

| | BNT55 | BNT60 | BNT65 | BNT70 |
|---|---|---|---|---|
| U (J/cm$^3$) | 42.1 | 48.1 | 49.3 | 51.5 |
| $U_{re}$ (J/cm$^3$) | 20.1 | 26.8 | 41.6 | 33.1 |
| $\eta$ (%) | 47.7 | 55.7 | 84.3 | 64.3 |

Journal of Applied Physics
ACCEPTED MANUSCRIPT
AIP Publishing
This is the author's peer reviewed, accepted manuscript. However, the online version of record will be different from this version once it has been copyedited and typeset.
PLEASE CITE THIS ARTICLE AS DOI: 10.1063/5.0005775

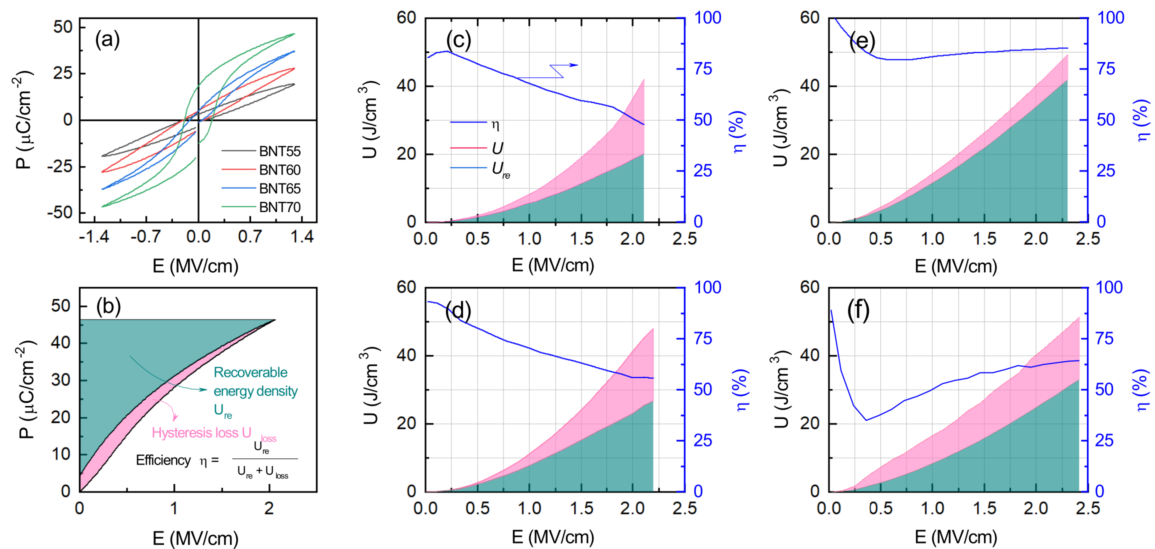


FIG. 3. The electric field dependent polarization hysteresis loops of (a) all BNT films and (b) the schematic diagram of energy storage density based on $P$-$E$ loops (the magenta and dark green area indicates $U_{loss}$ and $U_{re}$, respectively). The energy storage properties (include $U$, $U_{re}$, $\eta$) dependence on the applied electric field amplitude are given in the corresponding illustration (c) BNT55, (D) BNT60, (E) BNT65, (F) BNT70.

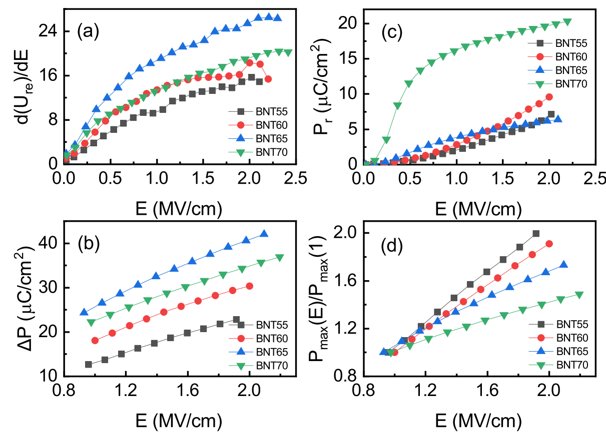


FIG. 4. (a) The derivative of $U_{re}$ with electric field for all BNT thin films. (b) and (c) Electric field dependence of the $P_r$ and $\Delta P$ of BNT films. (d) The $P_m$ normalized to the polarization at the field of 1 MV/cm as a function of electric field.

the Fig. 3(b). BNT65 film (also shows in the Fig. 3(e)) has the largest $U_{re}$, though the BNT70 has the highest $U$. BNT70 film has a serious $U_{loss}$ due to the significant hysteresis, as shown in the electric field dependence of the energy storage density of Fig. 3(f). This is adverse for energy storage capacitors because more heat is generated during the discharging process.[30] Compared with BNT70, BNT60 and BNT55 (show in Fig. 3(c) and (d)), BNT65 exhibits the narrowest magenta shaded area, e.g. $U_{loss}$, resulting in the optimal $U_{re}$. Fig. 3(c)-(f) also show that the increase in electric field to 0.5 MV/cm decreases the energy storage efficiency of all samples. This decrease in $\eta$ at $E < 0.5$ MV/cm is attributed to the appearance of remnant polarization. It is noted that $\eta$ drops near $E$ = 0.5 MV/cm in BNT65 and BNT70. This abrupt decrease in $\eta$ of BNT65 and BNT70 indicates that the increase in electric field dramatically increases remnant polarization near $E$ = 0.5 MV/cm which is close to the coercive field of ferroelectric BNT films. At $E > 0.5$MV/cm, the increase in electric field increases $P_m$ but has a marginal impact on $P_r$. Hence, the increase in electric field slightly increases $\eta$ of BNT65 and BNT70.

Fig. 4(a) shows d$U_{re}$/dE of four BNT films as a function of electric field, which reflects the faster growth rate of $U_{re}$ in BNT65. Thus, BNT65 film stores the most recoverable energy and possesses the highest energy storage efficiency. Following the formula of energy storage density of $U$ and $U_{re}$, it can be deduced that $P_r$ or more specifically a polarization drops $\Delta P$=$P_m - P_r$ is extremely important to achieve the high recoverable energy storage density. A large polarization drop $\Delta P$ is needed for high $U_{re}$. $\Delta P$ and $P_r$ of BNT films are shown in Fig. 4(b) and (c). $\Delta P$ of BNT65 and BNT70 is 42 $\mu$C/cm$^2$ and 35.6 $\mu$C/cm$^2$ at maximum electric field, respectively. This explains why BNT65 has a superior energy-storage efficiency $\eta$ of 84.3% with small $U_{loss}$. In Fig. 4(c), on one hand, dramatically increases in remnant polarization near $E$ = 0.5 MV/cm of BNT65 and BNT70 films, which result in abrupt decrease in $\eta$ discuss above. On the other hand, $P_r$ of BNT65 and BNT70 tend to be saturated at high electric field while $P_r$ of BNT50 and BNT55 increases as the electric field increases. These differences in $\Delta P$, $P_m$ and $P_r$ results in different response of $\eta$ to a change in electric field at $E > 0.5$ MV/cm. Fig. 4(d) shows the effect of electric field on normalized $P_m$ using $P_m$ at $E$ = 1 MV/cm. A slope of normalized $P_m-$ electric field curve is the smallest in BNT70, though it has the highest $P_m$ at a given electric field. This slow increase in $P_m$ limits the energy storage density of

Journal of Applied Physics
ACCEPTED MANUSCRIPT
AIP Publishing
This is the author's peer reviewed, accepted manuscript. However, the online version of record will be different from this version once it has been copyedited and typeset.
PLEASE CITE THIS ARTICLE AS DOI: 10.1063/5.0005775

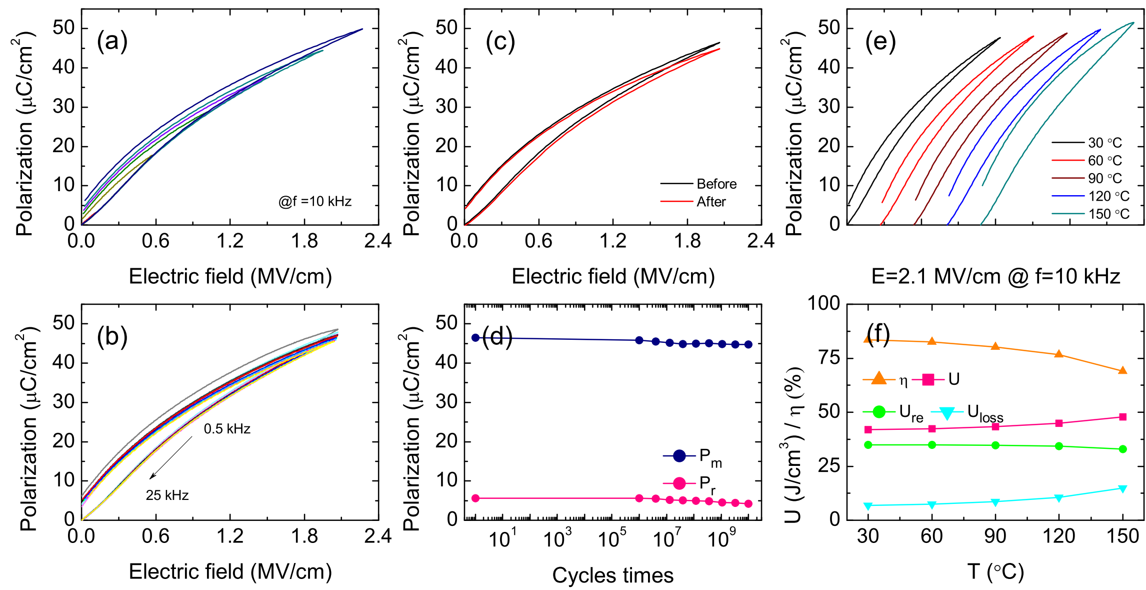


FIG. 5. The ferroelectric and energy storage stability of BNT65 thin films. (a) and (b) Evolution of polarization under electric field amplitude and applied frequency. (c) and (d) Given the $P$-$E$ hysteresis loops before and after $10^{10}$ switching cycles and corresponding $P_m$ and $P_r$ during the switching process. (e) and (f) The $P$-$E$ hysteresis loops and corresponding energy storage properties of BNT65 thin films at different temperature.

BNT70 at high electric field.[31] On the other side, BNT55 and BNT60 have a larger slope in normalized $P_m$ vs electric field. In BNT55 and BNT60, however, the magnitude of $P_m$ is small and the leakage current is high. This, in turn, limit the energy storage density of BNT55 and BNT60. Combined the smaller $P_r$, larger increase of normalized $P_m$ and smaller leakage current, BNT65 possesses the large $\Delta P$ and exhibits the best energy storage properties. The $U_{re}$ of 41.6 J/cm$^3$ is comparable to that of thin film dielectric energy storage capacitors of perovskite ferroelectric that are reported very recently.[1,32,34] However, $\eta$ of 84.3% in this study is certainly higher than $\eta$ in the recent reports.[9–13,19–21,32–36] The energy storage performance of AP compounds that are another important class of ferroelectrics, need more examination.[37] The enhancement of the energy storage performance of BNT thin films by simply controlling of the crystallization (or grain size) is a feasible and facile method to produce the dielectric energy storage devices.

In order to further systematically investigate the potential of BNT65 thin film for energy storage application, $P$-$E$ curve is measured at different frequencies and the stability of polarization is tested at different temperatures. The results of unipolar polarizations measurements are shown in Fig. 5 and a function of corresponding parametric variables and their energy storage properties are also demonstrated. Typical unipolar $P$-$E$ curves of ferroelectric materials are found as show in the Fig. 5(a), their polarization increases with the electric field amplitude increases. The narrow scimitar-type loops ensure low energy losses during the discharging process. Fig. 5(b) exhibits the unipolar polarizations-electric field loops with frequency range from 500 Hz to 25 kHz under the same field amplitude. As the measurement frequency increases, $P_m$ and $P_r$ decrease by 6.3% and 22.5%, respectively. A smaller hysteresis at the high frequency suggests that $\eta$ of BNT65 gets larger at the high frequency, which imply is more suitable for energy storage applications at high frequencies.[1] Fig. 5(c) shows the unipolar polarization-electric field hysteresis loops before and after the film is exposed to $10^{10}$ switching cycles. A changed in $P_m$ and $P_r$ during the switching process is also presented in Fig. 5(d). A marginal fatigue of maximum polarization is observed but remnant polarization does not show any attenuation. The energy storage density of 34.2 J/cm$^3$ and 32.5 J/cm$^3$ and the efficiency of 84% and 82.3% are calculated based on their loops before and after fatigue test, respectively. This demonstrate that such film capacitor has good fatigue endurance properties. From the formula of the energy storage, it is concluded that the separate reduction of remnant polarization helps to enhance the efficiency of ferroelectric capacitors. This is actually one of the key points of whether ferroelectrics can be used for dielectric capacitors. In general, the reduction of remnant polarization is accompanied by a decrease in maximum polarization and a deterioration in the insulation of the material.[38] In addition, the maximum polarization suffers from more serious loss, compared to the remnant polarization in most case.[28] This is exactly the plot occurred here and other reports.[19] However, it is very interesting that much ferroelectric energy storage capacitors reported so far have relatively good anti-fatigue characteristics, according to the above-mentioned fatigue test mode. When a ferroelectric film has a rectangular hysteresis loop characteristic, their is usually accompanied by polarization fatigue. In contrast, when the ferroelectric film has a narrow hysteresis loop, the film does not exhibit significantly polarization fatigue. This trend is obviously observed in the perovskite ferroelectrics, while

Journal of Applied Physics
ACCEPTED MANUSCRIPT
AIP Publishing
This is the author's peer reviewed, accepted manuscript. However, the online version of record will be different from this version once it has been copyedited and typeset.
PLEASE CITE THIS ARTICLE AS DOI: 10.1063/5.0005775

the layered perovskites are generally more fatigue-resistant. Therefore, it seems to be a way to reduce the remnant polarization of ferroelectrics and use it for dielectric energy storage. After all, the unusual phenomenon of polarization fatigue has been confirmed in hafnium oxide.[39]

Figure 5(e) shows the unipolar $P$-$E$ hysteresis loops of BNT65 thin films at different temperature. The shape of the loops gradually broadens as the measurement temperature increased signify that the switching properties have some dependence on the temperature. Both $P_m$ and $P_r$ keep increasing with the increase in the annealing temperature, which is different from previous reports in BFO-based ferroelectric energy storage capacitors prepared by pulsed laser deposition.[35] But this phenomenon is consistent with the previous reports in AP thin film capacitors prepared by chemical solution deposition.[19] Here, the polarization continues increasing from 30 to 150 °C with the increasing temperature. At high temperature, thermal energy causes easier movement and reversal of ferroelectric domains. In addition, the increase in the leakage current at higher temperature contributes to the polarization as well as the dielectric loss. The separation of two different effects needs further analysis. Ferroelectric energy storage performance of BNT65 film at different temperature is shown in Fig. 5(f). The efficiency of the BNT65 film gradually decreases from 83.5% to 69% as the measurement temperature increases from 30° to 150°. However, $U_{re}$ varies slightly from 35 J/cm$^3$ to 33 J/cm$^3$. This suggests that BNT65 film releases energy stably during the discharging process. With the increasing measurement temperature from 30 to 150 °C, $U$ and $U_{loss}$ increase from 41.9 J/cm$^3$ to 47.8 J/cm$^3$ and 6.9 J/cm$^3$ to 14.8 J/cm$^3$, respectively. This is because both $P_m$ and $P_r$ increase together over temperature and the ratio of $P_m/P_r$ decreases from 8.8 to 4.7. Consequently, $\eta$ becomes low at high temperature. However, even efficiency of $\sim$0.7 is comparable to that other layered perovskite-like and cubic perovskite thin-film energy storage capacitors.[1,10–13,19–21,32–36]

## IV. CONCLUSIONS

Lead-free BNT thin films are deposited on platinum coated silicon substrates by CSD route. The ferroelectric energy storage properties of BNT films are investigated and discussed from the aspect of the crystallinity. As the thermal annealing temperature increase, the crystallinity and grain size of films increase. This leads to the appearance of ferroelectric polarization. A narrow hysteresis loop with large $P_m/P_r$ and low leakage current are obtained in films annealed at the moderate temperature (650 °C), in comparison to its counterpart which are annealed at higher temperature (700 °C) and completely crystallized. Large $P_m/P_r$ and low leakage current enables the high energy storage density of 41.6 J/cm$^3$ and the remarkable storage efficiency of 84.3% at 2.3 MV/cm. Moreover, the BNT thin film shows the excellent fatigue endurance and good thermal stability with stable energy release during the discharging process. These results suggest that BNT thin film can be considered as lead-free ferroelectric capacitors in the energy storage applications.

This work was supported by National NSFC (Grants No. 51801077, No. 11847093), Guangdong Basic and Applied Basic Research Foundation (Grants No. 2019A1515110018), the Scientific Research Foundation of JUST (Grant No. 1052931611, 1052921801).

The data that support the findings of this study are available from the corresponding author upon reasonable request.

[1] H. Pan, F. Li, Y. Liu, Q. Zhang, M. Wang, S. Lan, Y. Zheng, J. Ma, L. Gu, Y. Shen, P. Yu, S. Zhang, L. Q. Chen, Y. H. Lin and C. W. Nan, Science **365**, 578 (2019).
[2] L. Yang, X. Kong, F. Li, H. Hao, Z. Cheng, H. Liu, J.-F. Li and S. Zhang, Prog. Mater Sci. **102**, 72 (2019).
[3] M. Rath, M. Miryala, M. Murakami and M. S. Ramachandra Rao, J. Phys. D: Appl. Phys. **52**, 304001 (2019).
[4] S. Li, H. Nie, G. Wang, C. Xu, N. Liu, M. Zhou, F. Cao and X. Dong, J. Mater. Chem. C **7**, 1551 (2019).
[5] Z. Cheng, M. Lin, S. Wu, Y. Thakur, Y. Zhou, D.-Y. Jeong, Q. Shen and Q. M. Zhang, Appl. Phys. Lett. **106**, 202902 (2015).
[6] D. S. Gyan, and A. Dwivedi, J. Appl. Phys. **125**, 024103 (2019).
[7] F. Liu, Q. Li, J. Cui, Z. Li, G. Yang, Y. Liu, L. Dong, C. Xiong, H. Wang and Q. Wang, Adv. Funct. Mater. **27**, 1606292 (2017).
[8] H. Huang and J. F. Scott, *Ferroelectric Materials for Energy Applications* (Wiley-VCH, Weinheim, 2018), p. 123.
[9] M. D. Nguyen, J. Eur. Ceram. Soc. **40**, 1886 (2020).
[10] V. S. Puli, D. K. Pradhan, I. Coondoo, N. Panwar, S. Adireddy, S. Luo, R. S. Katiyar and D. B. Chrisey, J. Phys. D: Appl. Phys. **52**, 255304 (2019).
[11] H. J. Lee, S. S. Won, K. H. Cho, C. K. Han, N. Mostovych, A. I. Kingon, S.-H. Kim and H. Y. Lee, Appl. Phys. Lett. **112**, 092901 (2018).
[12] Z. Sun, C. Ma, X. Wang, M. Liu, L. Lu, M. Wu, X. Lou, H. Wang and C. L. Jia, ACS Appl. Mater. Interfaces **9**, 17096-17101 (2017).
[13] C. Yang, Q. Yao, J. Qian, Y. Han and J. Chen, Ceram. Int. **44**, 9643 (2018).
[14] P. Lv, C. Yang, J. Qian, H. Wu, S. Huang, X. Cheng and Z. Cheng, Adv. Energy Mater. **10**, 1904229 (2020).
[15] C. Yang, J. Qian, Y. Han, P. Lv, S. Huang, X. Cheng and Z. Cheng, J. Mater. Chem. A **7**, 22366 (2019).
[16] C. Yang, J. Qian, P. Lv, H. Wu, X. Lin, K. Wang, J. Ouyang, S. Huang, X. Cheng and Z. Cheng, J. Materiomics **6**, 200 (2020).
[17] B. Xu, J. Iniguez and L. Bellaiche, Nat. Commun. **8**, 15682 (2017).
[18] J. Yang, D. Song, Y. Yin, L. Chen, L. Chen, Y. Wang and J. Wang, Mater. Sci. Eng. B-Adv. **248**, 114408 (2019).
[19] B. Yang, M. Guo, C. Li, D. Song, X. Tang, R. Wei, L. Hu, X. Lou, X. Zhu and Y. Sun, Appl. Phys. Lett. **115**, 243901 (2019).
[20] Z. H. Tang, J. Y. Chen, B. Yang and S. F. Zhao, Appl. Phys. Lett. **114**, 163901 (2019).
[21] X. Liu, S. Xue, F. Wang, J. Zhai and B. Shen, Acta Mater. **164**, 12 (2019).
[22] F. Yang, F. Zhang, G. Hu, Z. Zong and M. Tang, Appl. Phys. Lett. **106**, 172903 (2015).
[23] D. Song, J. Yang, B. Yang, L. Chen, F. Wang and X. Zhu, J. Mater. Chem. C **6**, 8618 (2018).
[24] S. Bhardwaj, J. P. Sharma, K. K. Raina and R. Kumar, AIP Conf. Proc. **1536**, 155 (2013).
[25] K. Seiji, I. Ryo, H. Shinichi and T. Masaaki, Jpn. J. Appl. Phys. **33**, 5559 (1994).
[26] L. -C. Zhang and L. -Y. Chen, Adv. Eng. Mater. **21**, 1801215 (2019).
[27] C. J. Lu, Y. Qiao, Y. J. Qi, X. Q. Chen and J. S. Zhu, Appl. Phys. Lett. **87**, 222901 (2005).
[28] D. Song, J. Yang and Y. Wang, Ceram. Int. **45**, 10080 (2019).
[29] D. William, D. Callister, and G. Rethwisch, *Materials Science and Engineering: An Introduction* (John Wiley & Sons, New York, 2009), p. 992.
[30] Q. Li, F. Liu, T. Yang, M. R. Gadinski, G. Zhang, L.-Q. Chen and Q. Wang, P. Natl. Acad. of Sci. USA **113**, 9995 (2016).
[31] L. Yang, X. Kong, Z. Cheng and S. Zhang, J. Mater. Chem. A **7**, 8573 (2019).
[32] J. Xie, H. Liu, Z. Yao, H. Hao, Y. Xie, Z. Li, M. Cao and S. Zhang, J. Mater. Chem. C **7**, 13632 (2019).
[33] Y. Hu, Q. Xie, R. Liang, X. Zhao, Z. Zhou, X. Dong, F. Wang, Y. Tang, N. Liu and X. Liu, AIP Adv. **9**, 085005 (2019).
[34] Q. Fan, C. Ma, Y. Li, Z. Liang, S. Cheng, M. Guo, Y. Dai, C. Ma, L. Lu, W.

Journal of Applied Physics ACCEPTED MANUSCRIPT
AIP Publishing
This is the author's peer reviewed, accepted manuscript. However, the online version of record will be different from this version once it has been copyedited and typeset.
PLEASE CITE THIS ARTICLE AS DOI: 10.1063/5.0005775

Wang, L. Wang, X. Lou, M. Liu, H. Wang and C.-L. Jia, Nano Energy **62**, 725 (2019).
[35] H. Pan, Y. Zeng, Y. Shen, Y.-H. Lin, J. Ma, L. Li and C.-W. Nan, J. Mater. Chem. A **5**, 5920 (2017).
[36] N. Sun, Y. Li, J. Liu and X. Hao, J. Power. Sources **448**, 227457 (2019).
[37] X. Li, Y. Sun, Q. Wu, H. Liu, W. Gu, X. Wang, Z. Cheng, Z. Fu and Y. Lu, J. Am. Chem. Soc. **141**, 3121 (2019).
[38] N. Zhong, P.-H. Xiang, Y.-Y. Zhang, X. Wu, X.-D. Tang, P.-X. Yang, C.-G. Duan and J.-H. Chu, J. Appl. Phys. **118**, 104102 (2015).
[39] S. Mueller, J. Mller,U. Schroeder and T. Mikolajick, IEEE T. Device Mat. Re. **13**, 93 (2013).

ACCEPTED MANUSCRIPT
Journal of Applied Physics
AIP Publishing
This is the author's peer reviewed, accepted manuscript. However, the online version of record will be different from this version once it has been copyedited and typeset.
PLEASE CITE THIS ARTICLE AS DOI: 10.1063/5.0005775

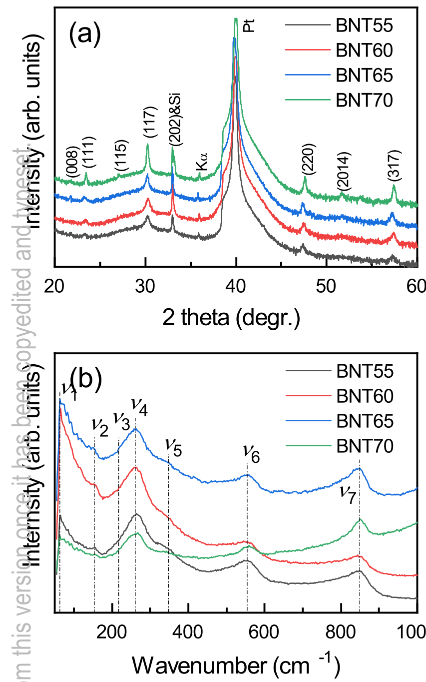


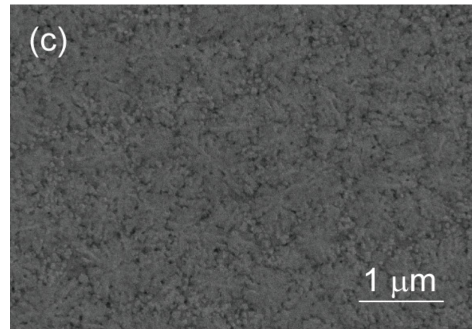


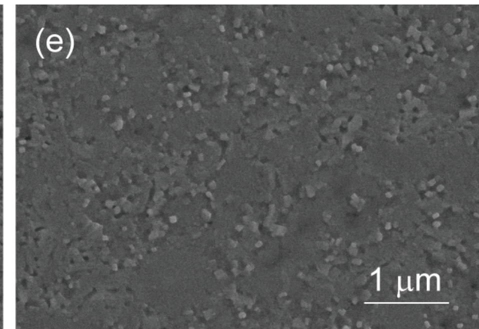


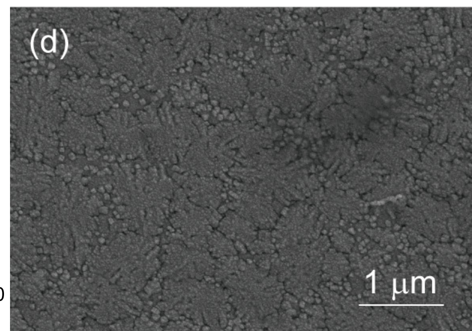


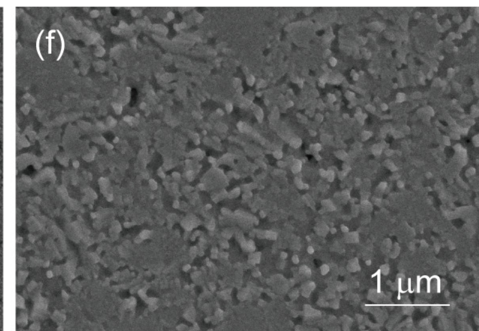

ACCEPTED MANUSCRIPT
Journal of Applied Physics
AIP Publishing
This is the author's peer reviewed, accepted manuscript. However, the online version of record will be different from this version once it has been copyedited and typeset.
PLEASE CITE THIS ARTICLE AS DOI: 10.1063/5.0005775

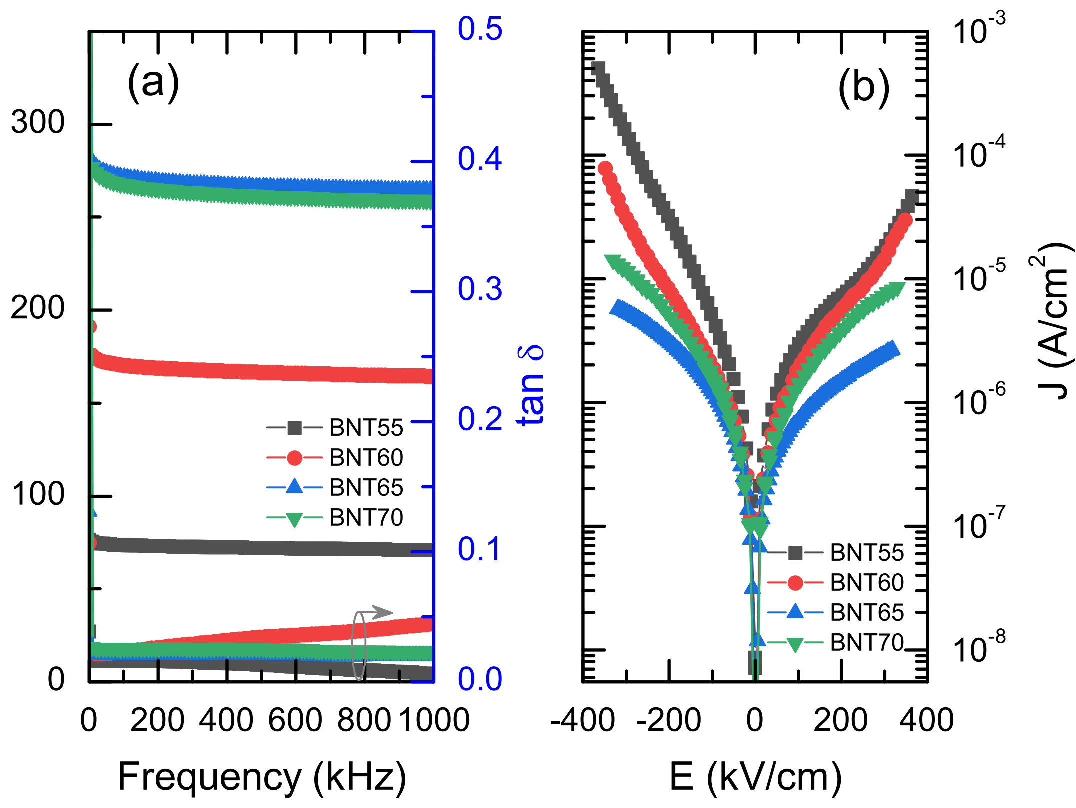

ACCEPTED MANUSCRIPT
Journal of Applied Physics
AIP Publishing
This is the author's peer reviewed, accepted manuscript. However, the online version of record will be different from this version once it has been copyedited and typeset.
PLEASE CITE THIS ARTICLE AS DOI: 10.1063/5.0005775

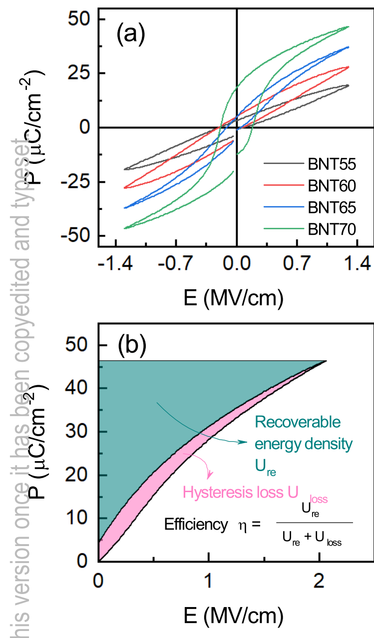


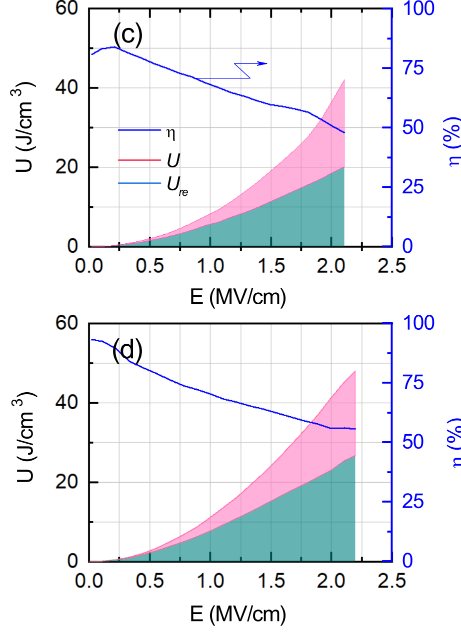


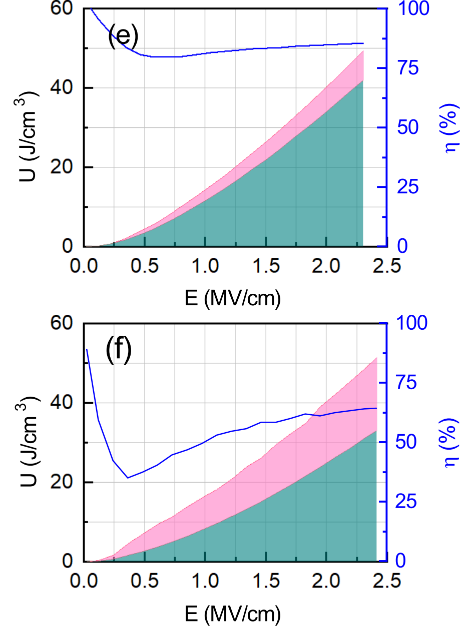

ACCEPTED MANUSCRIPT
Journal of Applied Physics
AIP Publishing
This is the author's peer reviewed, accepted manuscript. However, the online version of record will be different from this version once it has been copyedited and typeset.
PLEASE CITE THIS ARTICLE AS DOI: 10.1063/5.0005775

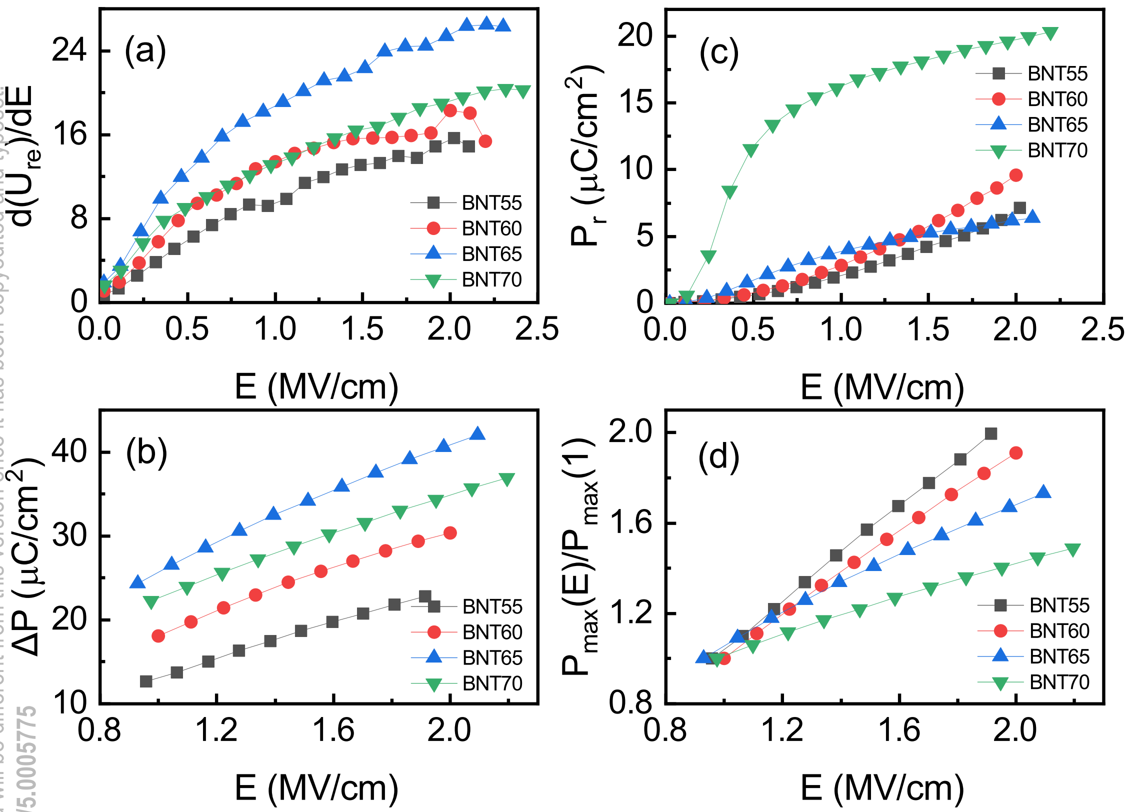

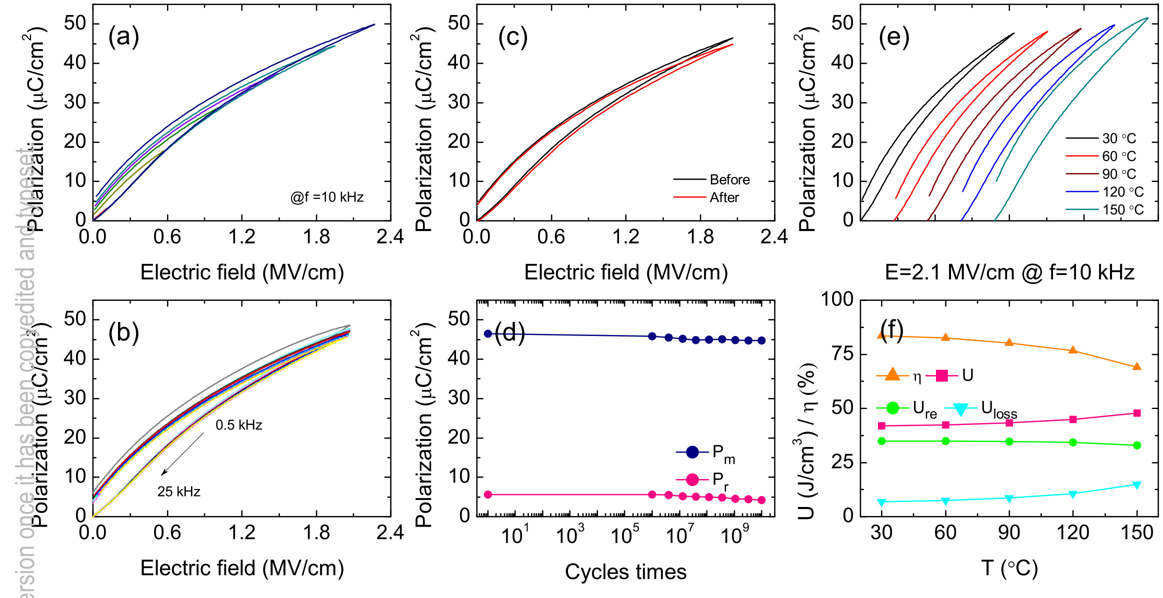


ACCEPTED MANUSCRIPT
Journal of Applied Physics
AIP Publishing
This is the author's peer reviewed, accepted manuscript. However, the online version of record will be different from this version once it has been copyedited and typeset.
PLEASE CITE THIS ARTICLE AS DOI: 10.1063/5.0005775